Sustainable Acoustic Insulation: Perforated Recycled PET Foam-Honeycomb Sandwich Structure with Improved Half-Absorption Bandwidth

S. Ravichandran[1,3], M. Hojjati[1,3], E.R Fotsing[2,3], A. Ross[2,3]
[1]Concordia Center for Composites (CONCOM), Montreal, Quebec, Canada
[2] Laboratory for Acoustics and Vibration Analysis (LAVA), Polytechnique Montreal, Montreal, Quebec, Canada
[3] Research Center for High Performance Polymer and Composite Systems (CREPEC), Montreal, Quebec, Canada

Abstract

Limited absorption bandwidth and lack of sustainable solutions remain key challenges in acoustic insulation building materials. While perforated metallic closed-cell foams have been studied to a limited extent, the acoustic performance of perforated recycled polyethylene terephthalate (r-PET) foam remains unexplored. This study presents the first experimental characterization of perforated r-PET foam. It demonstrates a novel multi-layer structure combining perforated r-PET foam with honeycomb sandwich having graded-microperforation facesheets. The honeycomb core is made of fully recyclable polypropylene while the facesheet is made of fiberglass/PP composite, a sustainable option compared to conventionally used brick masonry. Experimental testing of r-PET foam samples with perforation ratios of 2.6%, 3.7%, and 4.8% revealed tunable absorption peaks at 967-2100 Hz with less than one octave bandwidth. Finite element model simulations show that the complete multi-layer foam-honeycomb structure achieves a half-absorption bandwidth of 2450 Hz (1350-3800 Hz), while the honeycomb subsystem with optimized heterogeneous microperforated facesheets alone provides 1060 Hz bandwidth (990-2050 Hz). This represents a significant improvement over single-layer perforated foams while utilizing sustainable materials from the 19 million tons of annual PET waste. The design maintains thermal insulation properties through limited perforation (<5%) and offers superior manufacturability compared to hierarchical honeycomb structures. This work establishes perforated r-PET foam as a viable sustainable alternative for building acoustic applications.

Keywords: *Acoustic absorption, recycled PET foam, honeycomb structures, microperforated panels, sustainable materials, broadband absorption*

---

1. Introduction

The building sector accounts for 40% of global energy consumption and 43% of greenhouse gas emissions, driving demand for multifunctional materials that combine acoustic comfort with thermal efficiency [1]. Simultaneously, approximately 19 million tons of polyethylene terephthalate (PET) are produced annually for plastic bottles, with many entering waste streams the same year [2], [3]. This presents both a challenge and an opportunity for developing sustainable acoustic materials using recycled closed-cell r-PET foam. Existing acoustic absorption solutions face inherent trade-offs. Perforated closed-cell foams typically achieve half-absorption bandwidths of less than one octave, though first absorption peaks occur at low frequencies [4], [5]. Single-layered microperforated panels (MPPs) offer bandwidths up to 2.5 octaves, with multilayered configurations achieving even broader coverage [6], [7]. However, these systems lack thermal insulation properties critical for building applications. Recent investigations into hierarchical honeycomb structures demonstrate multiple resonance peaks and improved mechanical strength [8], yet their complexity limits practical manufacturing scalability. Rajendran et al. [9] achieved 550 Hz bandwidth using 29 dissimilar cylindrical resonators, while Zhang et al. [10] demonstrated 270 Hz bandwidth with Helmholtz resonators with embedded apertures—both approaches requiring intricate designs that are challenging for mass production. Despite growing interest in mechanical-acoustic optimization, two critical gaps remain: (1) the acoustic properties of perforated r-PET foam have not been experimentally characterized, and (2) no sustainable multifunctional designs simultaneously address acoustic performance, thermal insulation, and manufacturability. Though honeycomb structures offer effective thermal insulation [11], their thermal performance is not as efficient as closed-cell PET foams [12], [13]. This study addresses both gaps by presenting experimental investigation of perforated r-PET foam and proposing a novel multi-layer structure integrating r-PET foam with graded-perforation honeycomb cores and microperforated facesheets. The design achieves broadband absorption while preserving thermal properties through limited perforation ratios (<5%) and maintaining manufacturing simplicity through a single-layer honeycomb with optimized heterogenous perforations.

2. Materials and Methods

2.1 Experimental Investigation of Perforated r-PET foam

Primary experimental characterization of the perforated PET foam enables us to model its behavior for subsequent integration into the numerical model of the multilayer structure. Recycled PET foam samples supplied by Innovative Composite Products (I-C-P Inc.), a manufacturer specializing in sandwich structures with foam cores. The r-PET (ArmaPET GR) foam itself is manufactured by Armacell® from post-consumer plastic bottle waste. Three perforation ratios were investigated for a foam of 70 kg/m^3 density: $\varphi_{perf,3}$ = 4.8%, $\varphi_{perf,2}$ = 3.7%, and $\varphi_{perf,1}$ = 2.6%. A perforation pattern consisting of 1.6 mm-diameter holes arranged radially was produced by driving nails through the foam, as illustrated in Figure 1. Properties of 150 kg/m³ density foam used in subsequent numerical modelling include quasi-isotropic tetrakaidecahedron unit cell with the following degree of anisotropy – $r_z/r_y = 1.23$, $r_y/r_x = 1.2$, and $r_z/r_x = 1.37$; r_z = 717 µm. Sound absorption coefficient, a shown in Figure 2, were measured using a two-microphone impedance tube following ISO 10534-2 standard. Sample dimensions were Ø29 × 25 mm. The process was repeated for three different samples to obtain the uncertainty in measurements. The frequency range spans 500-6500 Hz with 1 Hz increments. Tests were performed at 23°C and 20% relative humidity. The numerical fit to the experimental measurements is subsequently used in the multilayered structure.

Figure 1: r-PET samples without perforation (left) and with 1.6mm diameter needles (right).

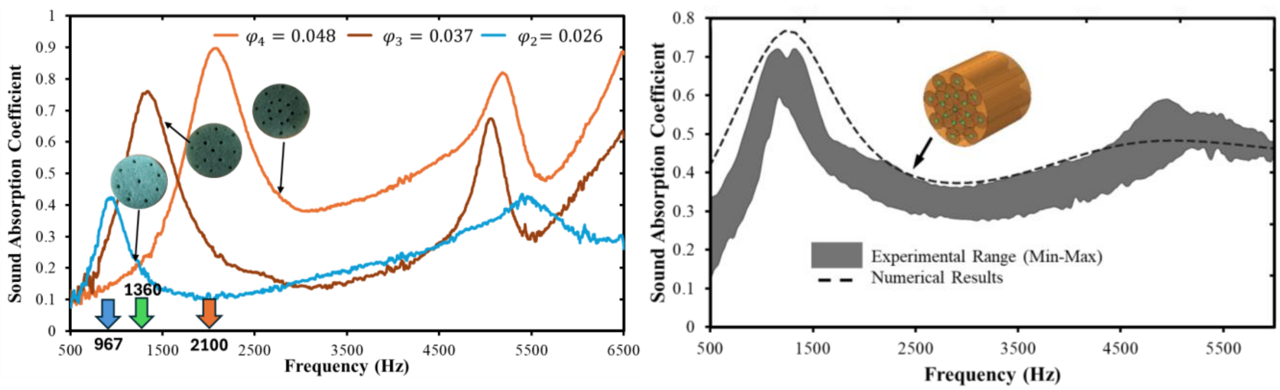

Figure 2: Sound absorption coefficient of perforated 70kg/m³ r-PET foam samples with increasing perforation density (left) numerical fitting of sound absorption coefficient of 150 kg/m³ sample (right).

2.2 Multi-layer Structure Design and Numerical Modeling

A 30-cell hexagonal array (42.5 × 32 mm) incorporates perforation diameter (d_p) ranging from 0.4 to 1.1 mm distributed across the panel. This grading strategy creates multiple overlapping resonances without requiring hierarchical honeycomb geometries, significantly simplifying manufacturing. The complete multi-layer structure comprises perforated r-PET foam, air cavity, and honeycomb core with uniform microperforated facesheets (Figure 3).

The detailed geometry and numerical modeling approach are described below. The proposed multi-layer structure consists of seven distinct components arranged sequentially from the incident sound side. Sound first encounters the air domain, followed by a microperforated facesheet with perforation radius $r_{f,h}$. Behind this lies the honeycomb core with length L_{h3} and cell size a'. This is followed by the back microperforated facesheet of thickness $L_{f,h}$ with perforation radius $r_{f,h}$, and an air cavity with gap length L_{g2}. The structure terminates with the perforated r-PET foam layer of length L_{f1} and perforation ratio φ ~ 5% and perforated facesheet of thickness $L_{f,f}$ on both the sides, with total structure length L. A one-at-a-time (OAT) sensitivity analysis was conducted to understand parameter influences on absorption characteristics. For each analysis, six parameters were held constant while two were varied systematically across their design ranges. Contour plots of average absorption coefficient from 500-3500 Hz versus parameter pairs revealed optimal design regions.

3D FE model was designed using COMSOL Multiphysics® v6.2. Thermo-viscous module was used for the honeycomb cores and the perforations while the air domain is modelled with Pressure Acoustics module. Sound hard boundary conditions were used for the lateral walls for the honeycomb cells with no-slip, isothermal conditions. A plane sound wave with a pressure amplitude of 1 Pa and a propagation speed of 343 m/s is introduced through a rectangular excitation port. 401255 extra fine tetrahedral domain elements, 50708 boundary elements and 4900 edge elements with 1528563 degrees of freedom were used for the 30-cell hexagonal array panel while 31424 domain elements, 108378 boundary elements, 22213 edge elements were used for the multilayer structure. Parametric sweep with 100 parametrized datapoints was used for each OAT sensitivity analysis.

Table 1: Geometric parameters of the multilayer structure post OAT analysis

	L_{f1} Foam Length (mm)	L_{g2} Air gap Length (mm)	L_{h3} Honeycomb Length (mm)	$L_{f,h}$ Facesheet Length – Honeycomb (mm)	$L_{f,f}$ Facesheet Length – Foam (mm)	$r_{f,h}$ Perforation radius – honeycomb facesheet (mm)	$r_{f,f}$ Perforation radius – foam facesheet (mm)
Post OAT	15	10	15	1	1	0.8	0.8

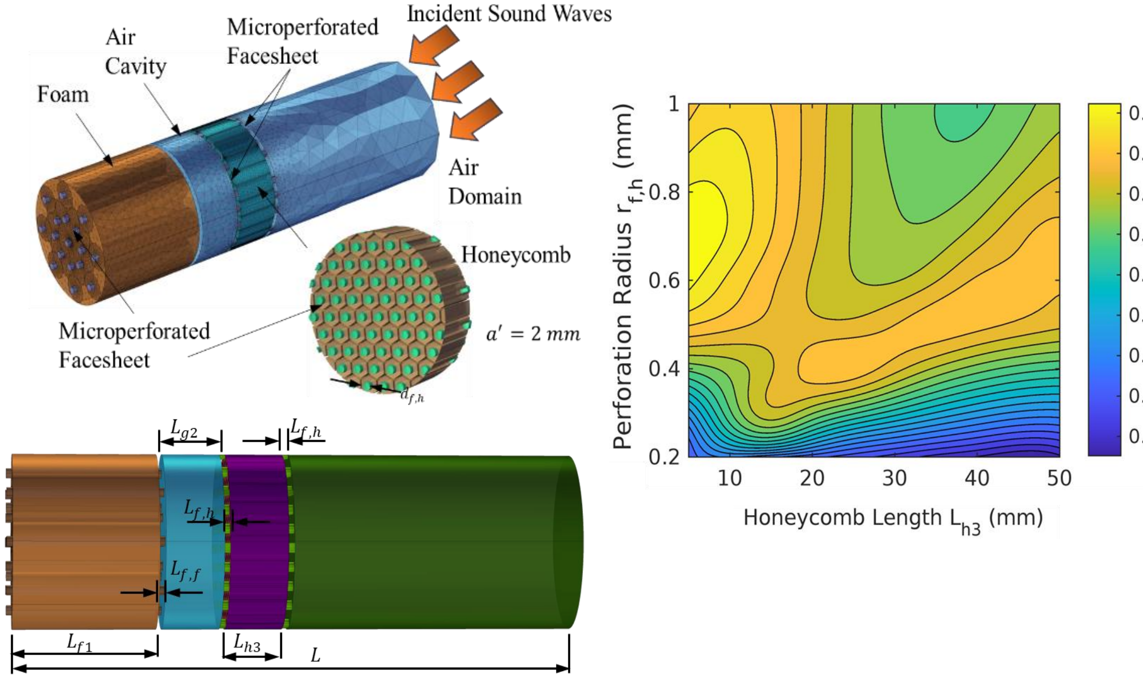

Figure 3: Multi-layer structure configuration (left) and parametric sensitivity of average absorption coefficient as a function of perforation radius and honeycomb length (right). L_{f1} *= 15 mm* L_{g2} *= 10 mm.*

3. Results

3.1 Honeycomb Structure with Optimized Graded Microperforations

Figure 4 presents the absorption coefficient as a function of frequency for the 30-cell honeycomb with the optimized graded microperforation distribution (black solid line) compared with the responses of the individual resonators (colored dashed lines). The honeycomb has cell size a = 4 mm, thickness T = 20 mm, while the facesheet has spatially distributed perforation radii ranging from 0.4 to 1.1 mm across the panel. The occupancy percentage for each perforation size was optimized to maximize broadband absorption. The combined structure achieves broadband absorption for a frequency range of 900-2175 Hz (half-absorption bandwidth = 1275 Hz) for $\alpha > 0.5$, 1100 Hz for $\alpha > 0.8$, and at multiple frequencies (1040, 1250, 1430, 1610, 1730, 1900, 2030, 2150 Hz) for $\alpha > 0.95$.

Larger perforation radii target higher frequencies (e.g., 1.1 mm → 2150 Hz), while smaller radii target lower frequencies (e.g., 0.4 mm → 1040 Hz). This is illustrated in Figure 5 which shows

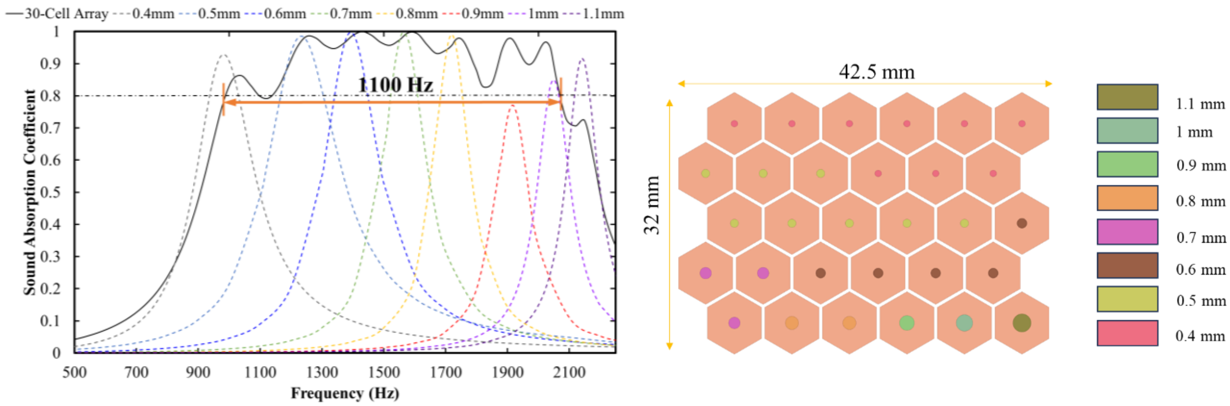

Figure 4: Absorption performance of optimized heterogeneous micro-perforated honeycomb panel. Spatial distribution of perforation diameters (color-coded: 0.4-1.1 mm) across the honeycomb array demonstrating the optimized occupancy distribution (right).

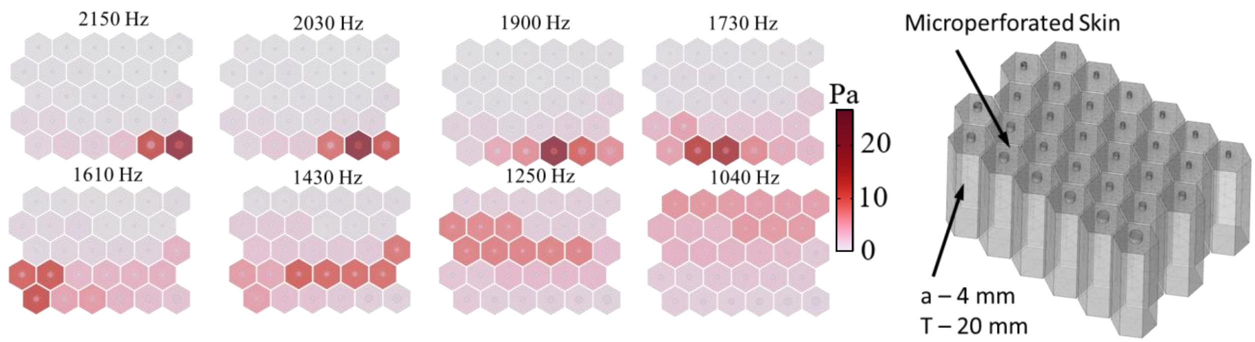

Figure 5: Root mean square (RMS) acoustic pressure distribution at resonance frequencies for different perforation diameters (1040-2150 Hz) (left). Three-dimensional honeycomb geometry (a' = 4 mm, T = 20 mm) (right).

the root-mean-square (rms) acoustic pressure at each resonance frequency corresponding to the associated perforation diameter. Resonance frequency of Helmholtz resonator can be calculated as –

$$f = \frac{C_0}{2\pi}\sqrt{\frac{\rho_0 S}{VM}}$$

Where C_0 and ρ_0 are the speed and density of sound, respectively, inside the resonator. S is the surface area of the neck, V is the volume of the resonator, and M is the inertial mass of the neck's air volume.

Since the resonance frequency depends on the surface area of the neck, different diameter perforations resonate at different frequencies. When the incident acoustic frequency and the resonance frequency of the cavity match, air particles oscillate at maximum intensity. The occupancy percentages (3-18%) were optimized to maximize broadband absorption. The thermo-viscous dissipation of sound energy, as illustrated in Figure 6, shows that larger perforation (d_p = 1.1 mm) has lower losses at 2150 Hz while smaller perforations (d_p = 0.4 mm) have higher losses at 1040 Hz. This explains the observed difference in the sound pressure level for different perforation sizes at their resonance frequencies.

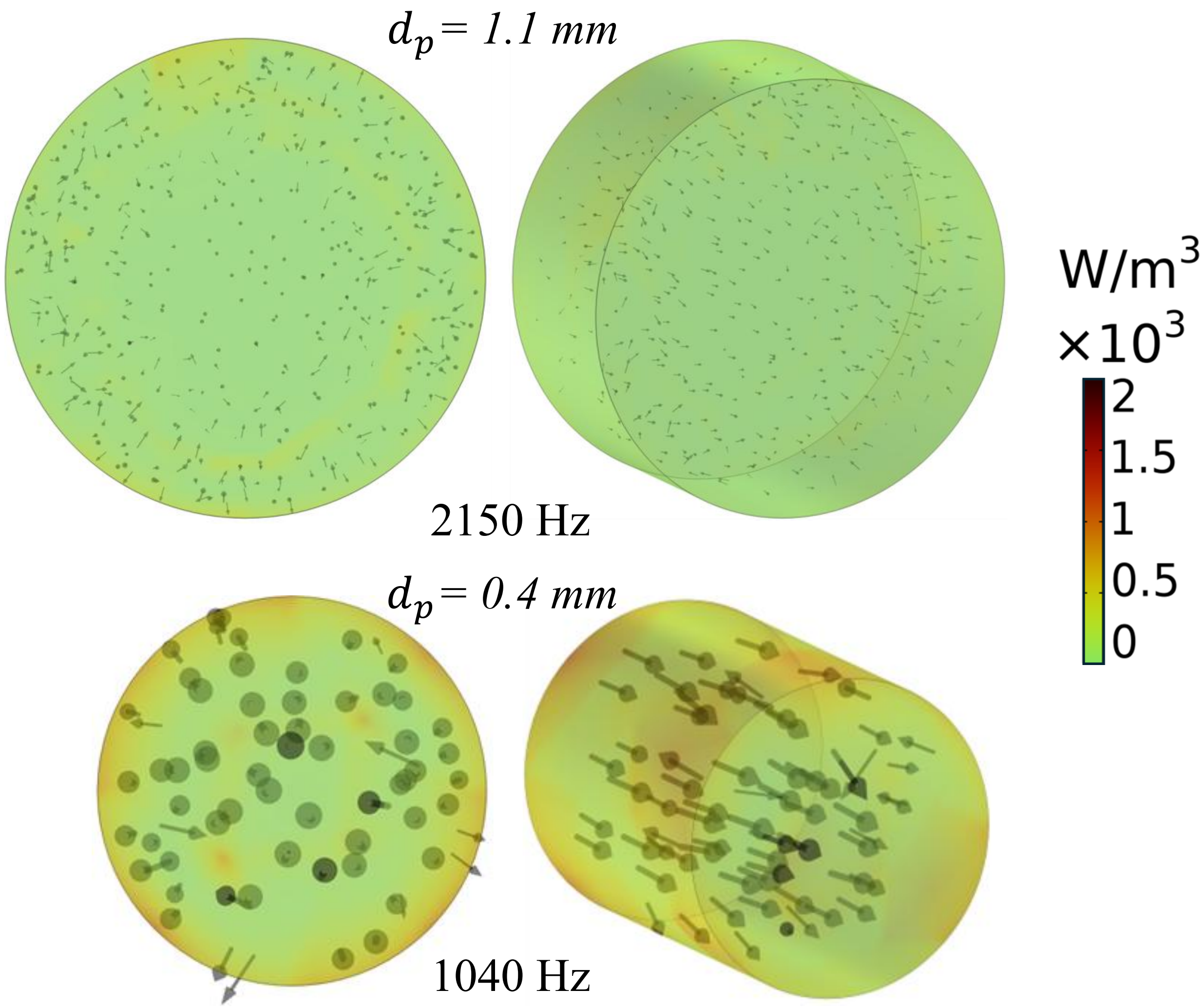

Figure 6: Total thermoviscous sound energy dissipation and sound intensity at their respective resonance frequencies. Color legend represents the thermoviscous dissipation while the arrows represent the sound intensity. Size scaled for better visualization

3.2 Parametric Sensitivity Analysis

Based on experimental characterization, r-PET foam with φ = 4.8% was integrated into the multi -layer structure to investigate broadband absorption potential. Sensitivity analyses revealed complex parameter interactions: with L_{f1} = 15 mm and L_{g2} = 10 mm fixed, perforation radius strongly influences absorption – $r_{f,h}$ values of 0.6-0.8 have highest average absorption of 0.7. With L_{g2} = 10 mm and r_f, h = 0.8 mm held constant, the absorption coefficient drops significantly when the foam length falls below a certain threshold. High absorption (α > 0.65) occurs for L_{f1} = 15-20 mm across honeycomb lengths of 5-10 mm (Figure 7). With L_{f1} = 15 mm and r_f, h = 0.8 mm fixed, absorption coefficient contours show best performance at $L_{g2} \approx$ 5-10 mm and $L_{h3} \approx$ 5-10 mm, achieving α ≈ 0.65-0.7. This highlights the influence of the air gap and the honeycomb length (Figure 7). Above a particular air gap, absorption coefficient significantly drops. The sensitivity analyses demonstrate that multiple resonance mechanisms interact synergistically. The foam provides low-frequency absorption while the honeycomb provides multiple mid-to-high frequency peaks.

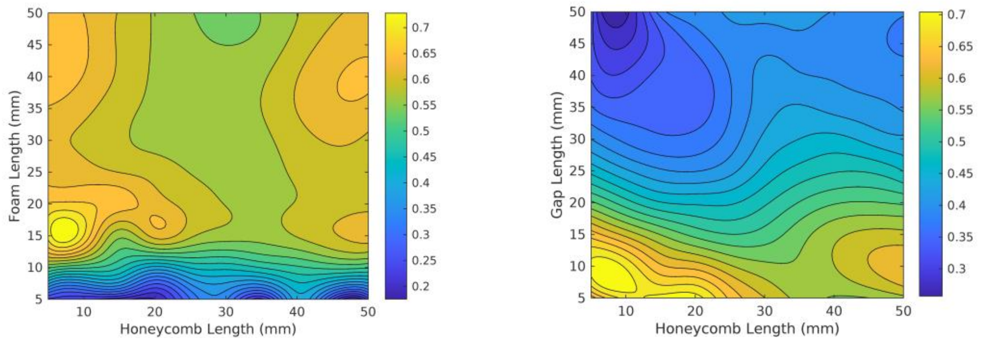

Figure 7: Contour plot of average absorption coefficient as a function of foam length (L_{f1}) and honeycomb length (L_{h3})(L_{g2}=10 mm and $r_{f,h}$=0.8 mm) (left), air gap length (L_{g2}) and honeycomb length (L_{h3})(L_{f1}=15 mm and $r_{f,h}$=0.8 mm) (right).

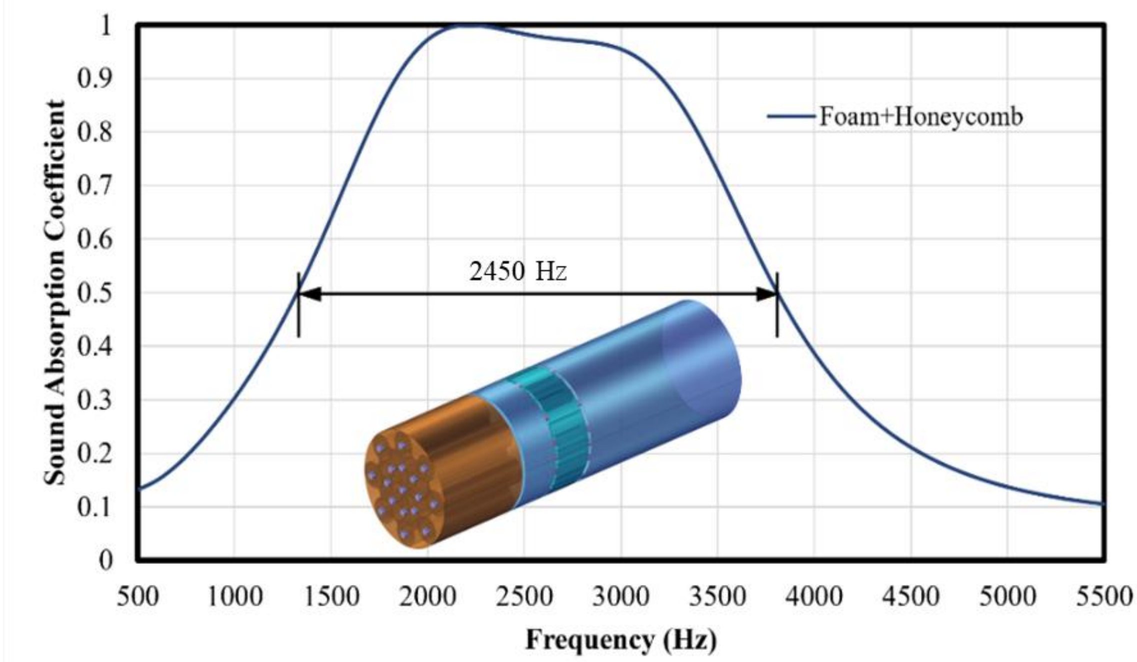

Figure 8: Sound absorption coefficient of hybrid r-PET foam and honeycomb structure.

Figure 8 presents the absorption performance of the complete integrated structure combining the perforated r-PET foam layer with the optimized uniform-perforation honeycomb. The dimensions are tabulated in Table 1. Complete structure performance shows a half-absorption bandwidth ($\alpha >$ 0.5) of 2450 Hz spanning 1350-3800 Hz and reaches peak absorption ($\alpha \approx 0.95$-1.0) over the 2000-3500 Hz frequency range**.** The combined bandwidth of 2450 Hz represents a significant improvement over the constituent components with 110% increase over the honeycomb alone (1275 Hz) and >2× improvement over single-layer r-PET foam (∼1000 Hz). As tabulated in Table 2, the multilayered structure outperforms the perforated aluminum foam significantly for approximately the same thickness.

Performance relative to the hierarchical honeycomb is slightly higher, but this comes at the cost of a substantial increase in overall thickness. In contrast, the multilayer structure remains far less complex to manufacture and offers strong sustainability advantages, including the added benefit of thermal insulation Both the 29 dissimilar resonators and the HREA configuration exhibit a narrower absorption bandwidth—shifted toward lower frequencies—while also involving very high structural complexity and poor sustainability, making them less attractive design options. The single-layer MPP outperforms the multilayer structure, achieving a 2500 Hz absorption bandwidth at a thickness of only 11 mm. This presents a unique opportunity to study as a future work the effect of combining both the graded perforations in the facesheets, and the hybrid r-PET foam and honeycomb structure to further improve the performance while maintaining the other desirable properties of low complexity, high sustainability.

Table 2: Comparison of half-absorption bandwidth of similar resonant structures.

Structure	Bandwidth	Thickness	Peak α	Complexity	Sustainability
Perforated Al foam [4,5]	<1 octave	50, 26.4	0.8	Low	Low
Single-layer MPP [6]	Up to 2.5 octaves (~2500 Hz)	11	0.9	Low	Medium
Hierarchical honeycomb [8]	2054 Hz (621-2675 Hz)	25	0.9	High	Low
29 dissimilar resonators [9]	560 Hz (300-860 Hz)	-	0.95	Very high	Low
HREA [10]	270 Hz	43	~1.0	High	Low
r-PET foam (single layer)	<1 octave (~1000 Hz)	25	0.75	Low	High
Honeycomb + graded MPP	1275 Hz (900-2175 Hz)	22	>0.95	Low	Medium
Foam + Honeycomb (This work)	2450 Hz (1350-3800 Hz)	52	~1.0	Low	High

4. Conclusions

This study presents the experimental characterization of perforated r-PET foam, demonstrating tunable absorption peaks (967-2100 Hz) with perforation ratios of 2.6-4.8%. The complete multi-layer foam-honeycomb structure achieves 2450 Hz half-absorption bandwidth (1350-3800 Hz), comparable to multi-layer MPP systems. Key advantages include: (1) sustainability through utilization of recycled PET from 19 million tons annual waste, (2) multifunctionality combining acoustic absorption with thermal insulation (perforation <5%), (3) simplicity using uniform array of honeycomb core rather than complex hierarchical designs, and (4) performance superior to single-layer perforated foams (>2× bandwidth improvement).

Acknowledgment

Gratitude is expressed to the invaluable contributions of Dr. Manuel Flores Salinas at Polytechnique Montreal, NSCERC, and Mr. Heng Wang at CONCOM, Concordia University.

References

[1] M. J. SheikhMozafari, E. Taban, P. Soltani, M. Faridan, and A. Khavanin, "Sound absorption and thermal insulation performance of sustainable fruit stone panels," *Applied Acoustics*, vol. 217, p. 109836, Feb. 2024, doi: 10.1016/j.apacoust.2023.109836.

[2] K. Bocz *et al.*, "Recycled PET foaming: Supercritical carbon dioxide assisted extrusion with real-time quality monitoring," *Advanced Industrial and Engineering Polymer Research*, vol. 4, no. 3, pp. 178–186, Jul. 2021, doi: 10.1016/j.aiepr.2021.03.002.

[3] Y. Gu *et al.*, "Environmental performance analysis on resource multiple-life-cycle recycling system: Evidence from waste pet bottles in China," *Resources, Conservation and Recycling*, vol. 158, p. 104821, Jul. 2020, doi: 10.1016/j.resconrec.2020.104821.

[4] K. C. Opiela, T. G. Zieliński, T. Dvorák, and S. Kúdela Jr., "Perforated closed-cell aluminium foam for acoustic absorption," *Applied Acoustics*, vol. 174, p. 107706, Mar. 2021, doi: 10.1016/j.apacoust.2020.107706.

[5] F. Chevillotte, C. Perrot, and R. Panneton, "Microstructure based model for sound absorption predictions of perforated closed-cell metallic foams," *The Journal of the Acoustical Society of America*, vol. 128, no. 4, pp. 1766–1776, Oct. 2010, doi: 10.1121/1.3473696.

[6] H. Ruiz, P. Cobo, and F. Jacobsen, "Optimization of multiple-layer microperforated panels by simulated annealing," *Applied Acoustics*, vol. 72, no. 10, pp. 772–776, Oct. 2011, doi: 10.1016/j.apacoust.2011.04.010.

[7] S. Yan, J. Wu, J. Chen, Y. Xiong, Q. Mao, and X. Zhang, "Optimization design and analysis of honeycomb micro-perforated plate broadband sound absorber," *Applied Acoustics*, vol. 186, p. 108487, Jan. 2022, doi: 10.1016/j.apacoust.2021.108487.

[8] W. He, X. Peng, F. Xin, and T. J. Lu, "Ultralight micro-perforated sandwich panel with hierarchical honeycomb core for sound absorption," *Jnl of Sandwich Structures & Materials*, vol. 24, no. 1, pp. 201–217, Jan. 2022, doi: 10.1177/1099636221993880.

[9] V. Rajendran, A. Piacsek, and T. Méndez Echenagucia, "Design of broadband Helmholtz resonator arrays using the radiation impedance method," *J Acoust Soc Am*, vol. 151, no. 1, p. 457, Jan. 2022, doi: 10.1121/10.0009317.

[10] J. Zhang, T. Chen, F. Xin, J. Zhu, and W. Ding, "New-parallel connection of the Helmholtz resonator with embedded apertures for low-frequency broadband sound absorption," *Japanese Journal of Applied Physics*, vol. 61, no. 7, p. 077001, Jul. 2022, doi: 10.35848/1347-4065/ac7761.

[11] S. Ravichandran and M. Hojjati, "Experimental and numerical thermal characterization of honeycomb core sandwich structures with glass/polypropylene twill weave composite face sheets," *International Journal of Heat and Mass Transfer*, vol. 231, p. 125869, Oct. 2024, doi: 10.1016/j.ijheatmasstransfer.2024.125869.

[12] J. Gu *et al.*, "Mechanical robust and thermal insulated rPET microcellular foam via supercritical CO2 foaming cross-linked photovoltaic backsheet," *Journal of CO2 Utilization*, vol. 97, p. 103126, Jul. 2025, doi: 10.1016/j.jcou.2025.103126.

[13] H. W. Koh *et al.*, "Advanced Recycled Polyethylene Terephthalate Aerogels from Plastic Waste for Acoustic and Thermal Insulation Applications," *Gels*, vol. 4, no. 2, p. 43, 2018, doi: 10.3390/gels4020043.